Plant Physiology and Biochemistry 111 (2017) 266–273

Contents lists available at ScienceDirect

Plant Physiology and Biochemistry

journal homepage: www.elsevier.com/locate/plaphy

Research article

Use of *Nicotiana tabacum* transplastomic plants engineered to express a His-tagged CP47 for the isolation of functional photosystem II core complexes

Cristina Pagliano [a, *], Luca Bersanini [b, 1], Rino Cella [b], Paolo Longoni [b, 2], Laura Pantaleoni [b, 3], Abhishek Dass [c], Sadhu Leelavathi [c], Vanga Siva Reddy [c, **]

[a] *Applied Science and Technology Department—BioSolar Lab, Politecnico di Torino, Viale Teresa Michel 5, 15121 Alessandria, Italy*
[b] *Department of Biology and Biotechnology, University of Pavia, Via Ferrata 9, 27100 Pavia, Italy*
[c] *Plant Transformation Group, International Center for Genetic Engineering and Biotechnology, Aruna Asaf Ali Marg, New Delhi 110067, India*

ARTICLE INFO

Article history:
Received 29 August 2016
Received in revised form
4 November 2016
Accepted 4 December 2016
Available online 8 December 2016

Keywords:
Biolistic chloroplast transformation
CP47 His-tag
Photosystem II
Transplastomic tobacco plants

ABSTRACT

This work focuses on the development of a molecular tool for purification of Photosystem II (PSII) from *Nicotiana tabacum* (L.). To this end, the chloroplast *psbB* gene encoding the CP47 PSII subunit was replaced with an engineered version of the same gene containing a C-terminal His-tag. Molecular analyses assessed the effective integration of the recombinant gene and its expression. Despite not exhibiting any obvious phenotype, the transplastomic plants remained heteroplasmic even after three rounds of regeneration under antibiotic selection. However, the recombinant His-tagged CP47 protein associated in vivo to the other PSII subunits allowing the isolation of a functional PSII core complex, although with low yield of extraction. These results will open up possible perspectives for further spectroscopic and structural studies.

1. Introduction

Photosystem II (PSII) is a multisubunit protein complex embedded in the thylakoid membranes of oxygenic photosynthetic organisms, where it performs a series of light-induced electron transfer reactions leading to the splitting of water into protons and molecular oxygen. The core complex of PSII is composed of about 16–17 intrinsic proteins and 3–4 extrinsic polypeptides encoded by *psb* genes, most of which, in the case of eukaryotic photosynthetic organisms (plants and algae), are plastidial and the remainder nuclear (Pagliano et al., 2013). It contains several cofactors, including chlorophylls, pheophytins, carotenoids, a heme, plastoquinones, lipids, as well as the Mn_4CaO_5 metallo cluster, which is the site of water oxidation (for the highest resolution structures available of cyanobacterial and plant PSII see (Umena et al., 2011; Wei et al., 2016)). It has been widely believed that the PSII core complex normally functions as a dimer and the monomeric complex may be an intermediate form in the normal assembly pathway or in the damage-repair cycle (Barbato et al., 1992; Hankamer et al., 1997; Danielsson et al., 2006). In each monomer, four large intrinsic subunits, namely D1 (PsbA) and D2 (PsbD), binding most of the redox cofactors forming the electron transport chain, and CP47 (PsbB) and CP43 (PsbC), functioning as inner antenna proteins, together with the small intrinsic α and β subunits (PsbE and PsbF) of cytochrome b_{559}, form the reaction centre (RC) of PSII. The RC is present in all oxygenic photosynthetic organisms and is plastome-encoded in eukaryotes. In the PSII core there are also several integral membrane subunits with low molecular mass (<10 kDa), accounting for more than half of the entire complex (Shi and Schröder, 2004; Shi et al., 2012). Although plant PSII has a core complex similar to that of cyanobacterial PSII, there are major differences in their lumenal extrinsic domains stabilizing

---

Abbreviations: HEPES, 4-(2-hydroxyethyl)-1-piperazineethanesulfonic acid; MES, 2-(N-morpholino)ethanesulfonic acid; Ni-NTA, nickel-nitrilotriacetic acid.

* Corresponding author.

** Corresponding author.

E-mail addresses: cristina.pagliano@polito.it (C. Pagliano), vsreddy@icgeb.res.in (V.S. Reddy).

[1] Present address: Department of Biochemistry, Molecular Plant Biology, University of Turku, FI-20014 Turku, Finland.

[2] Present address: Department of Botany and Plant Biology, University of Geneva, 30 Quai Ernest Ansermet, Sciences III, CH-1211 Genève, Switzerland.

[3] Present address: Department of Life Sciences and Biotechnology, University of Ferrara, Corso Ercole I d'Este 32, 44121 Ferrara, Italy.

http://dx.doi.org/10.1016/j.plaphy.2016.12.009
0981-9428/© 2016 Elsevier Masson SAS. All rights reserved.

the oxygen-evolving complex (OEC) which contains the Mn_4CaO_5 cluster (subunits PsbO, PsbP, and PsbQ, *vs*. PsbO, PsbU, and PsbV), and in their peripheral antenna systems (intrinsic light harvesting complexes LHCIIs *vs*. extrinsic phycobilisomes). Moreover, in the plant PSII core there are at least two small subunits that are not present in cyanobacteria, the intrinsic PsbW and the extrinsic PsbR.

The highest resolution at which the crystal structure of cyanobacterial PSII has been solved is 1.9 Å (Umena et al., 2011), after a decade-long optimization process starting from 3.8 Å resolution (recently reviewed in Shen (2015)). The structures of plant PSII core complexes have been firstly solved through cryo-electron crystallography at 8–10 Å resolution (Rhee et al., 1998; Hankamer et al., 1999, 2001). X-ray structures of isolated plant LHCII are available at 2.5–2.8 Å resolution (Liu et al., 2004; Standfuss et al., 2005; Pan et al., 2011) and of OEC subunits at 1.5–2.0 Å (Calderone et al., 2003; Ifuku et al., 2004; Balsera et al., 2005). More recently, details of the structure of a plant PSII-LHCII supercomplex obtained by cryo-electron microscopy at 3.2 Å resolution have been reported (Wei et al., 2016), marking a new step-forwards towards comprehension of the specific interactions between different PSII components. All these studies have resolved the basic structure of the plant PSII core complex and its associated pigment-protein complexes in higher plants. Now, optimization efforts are needed to achieve the detailed descriptions of specific structures within the plant PSII complex, as for example, the lumenal protein environment interacting with the Mn_4CaO_5 cluster known to be different in higher plants with respect to cyanobacteria, to underpin details of the water-splitting reaction, which supplies our atmosphere with the oxygen that we breathe. In this effort, isolation of an intact and functional PSII core complex of higher plants to study its structure-function relationships on a routine basis still remains a major and challenging task. Previously, Leelavathi and Reddy (2003) demonstrated, for the first time, the feasibility of over expressing a His-tagged recombinant protein in higher plant plastids through chloroplast genetic engineering approach and its subsequent purification using the ligand Ni-NTA system. This method has been successfully applied by several other groups for the purification of recombinant proteins from transplastomic plants and green algae (Johnson et al., 2007; Fey et al., 2008). Therefore, the aim of the present work was to extend this approach to tobacco plants by adding a 8x His-tag to one of the PSII core subunits and develop a protocol for an easy purification of the entire and functional PSII core complex. The strategy we adopted relies on the translational fusion of eight codons coding for histidine to the plastidial *psbB* gene encoding the CP47 protein. However, the challenge in this case is to insert the His-tag in a position that does neither alter the protein folding nor interfere with posttranslational modifications, if any, thus producing a recombinant protein retaining native functions and dynamics in order to get a biologically active PSII complex. Functional His-tagged CP47 proteins have been previously produced in the cyanobacterium *Synechocystis* sp. PCC6803 (Bricker et al., 1998; Kashino et al., 2002) and in the green alga *Chlamydomonas reinhardtii* (Suzuki et al., 2003), thus supporting the feasibility of this approach in higher plants. Despite several cycles of plant segregation and regeneration, we could not achieve complete homoplasmy for the transplastome containing a chimeric *psbB* gene to which a His-tag sequence was added; nevertheless, our approach resulted in the successful production of transplastomic plants accumulating a significant amount of PSII having His-tagged CP47 protein, which was sufficient to pull down PSII particles using Ni-NTA ligand. The isolated PSII complex was found to contain all the main PSII core intrinsic subunits and the extrinsic proteins PsbO, PsbP and PsbQ, and was active in evolving O_2 when tested under in vitro conditions. Taken together, these results demonstrate the feasibility of our approach for the isolation of a functional PSII core complex from transplastomic tobacco plants that might facilitate further structural and functional studies of higher plant PSII.

2. Materials and methods

2.1. Transformation vectors for the expression of recombinant genes encoding N– or C-terminal His-tagged CP47 protein in tobacco chloroplasts

The plastid transformation vectors pVSRCP47HisN and pVSRCP47HisC were generated using a Polymerase Chain Reaction (PCR) based approach. Primers were designed to contain the desired restriction sites for cloning each of the genetic elements and modified *psbB* gene into pVSR326 (GenBank Acc. No. AF527485) vector. An 8x His-tag along with a glycine linker (Gly-Gly-Gly-Gly) were fused to CP47 either at the N-terminus or C-terminus for efficient purification of the PSII complex. All the primers used in the cloning or PCR reactions are included in Table S1. The region upstream *psbB* gene, containing part of *clpP*, was amplified using CP47-5A HindIII and CP47-3A SacI primers using tobacco genomic DNA as a template. The resulting PCR product was digested with HindIII and SacI and ligated to pVSR326 digested with the same enzymes to create pVSRclpP vector. In the next step, the *psbB* gene was amplified with CP47-5Ba and CP47-3Ba primers or CP47-5Bb and CP47-3Bb primers to generate CP47His-BEG and CP47His-END DNA fragments, respectively. The CP47-5Ba primer was designed to introduce a 8x His-tag at the N-terminus of CP47 and the CP47-3Bb primer to add a similar His-tag fusion at the C-terminus. The PCR fragments CP47His-BEG and CP47His-END were digested with SacI and KpnI and ligated to pVSRclpP vector digested with the same restriction enzymes to create pVSRclpP:CP47HisBEG and pVSRclpP:CP47HisEND vectors, respectively. In the next step, a 326 bp *Oryza sativa psbA* 3′ Untranslated Region (UTR) was PCR amplified from the pVSR326 vector using PsbARterm5 and PsbARterm3 primers. The PCR product was digested with KpnI and ligated to pVSRclpP:CP47HisBEG and pVSRclpP:CP47HisEND vectors digested with KpnI to create intermediate vectors pVSRclpP:CP47HisBEGT and pVSRclpP:CP47HisENDT, respectively. The vectors having correct orientation of the *psb*A 3' UTR were selected by PCR using orientation specific primers and later confirmed by sequencing. In the final step, the *acc*D flanking region, present in the original pVSR326 vector, was replaced with CP47 FLKR region having *psbT*, *psbN*, *psbH* and a part of *petB* gene sequences using a PCR approach. The CP47 FLKR region was PCR amplified using CP47FLKRXho5 and CP47FLKRSal3 primers. The PCR product was digested with XhoI and SalI and ligated to pVSRclpP:CP47HisBEGT and pVSRclpP:CP47HisENDT vectors digested with XhoI and treated with alkaline phosphatase to create the final transformation vectors pVSRCP47HisN and pVSRCP47HisC, respectively.

2.2. Generation of transplastomic lines expressing modified CP47

The particle delivery method described previously by Leelavathi and Reddy (2003) was followed to generate stable transplastomic tobacco (*Nicotiana tabacum* L. cv. Petit Havana) plants. Standard procedures were followed to confirm stable integration and expression of transgenes in the transplastomic plants (Sambrook et al., 1989). PCR was used to identify the putative transplastomic lines regenerated on spectinomycin (500 mg L^{-1}) containing RMOP medium (Leelavathi et al., 2003). Three rounds of regeneration on spectinomycin selection were carried out to select homo-transplastomic plants.

2.3. Molecular characterization of transplastomic plants expressing modified CP47

Plants confirmed positive for the presence of modified *psbB* gene and selection (*aadA*) gene in the PCR analysis were further analyzed by Southern blot analysis to confirm the site-specific integration and the replacement of native wild-type *psbB* with *psbB*HisN or *psbB*HisC gene, depending on the construct used. Total genomic DNA isolated from different independently transformed lines was digested with EcoRV and SpeI, electrophoresed on 0.8% agarose gels and blotted onto Hybond-N+ membrane. Blots were probed with the coding region of *psbB*.

2.4. Thylakoid isolation from soil-grown plants

Transplastomic tobacco plants were transferred from culture boxes to the soil and grown for ten weeks inside a growth chamber (SANYO MLR-351H), at 20 °C, 60% humidity under a light regime of 8 h light and 16 h darkness per day, with a light intensity of 150 μmol m^{-2} s^{-1} photons. The same growth conditions were used for wild-type plants.

For thylakoids extraction, tobacco leaves were homogenized in 50 mM HEPES pH 7.5, 300 mM sucrose, 5 mM $MgCl_2$ and 6% (w/v) polyvinylpyrrolidone in a ratio 100 g fresh leaves:200 mL buffer. The homogenate was filtered on four layers of cotton cloth and membranes sedimented by centrifugation at 1500*g* for 10 min. Resulting pellets were washed once by centrifugation in the same buffer. Pellets were resuspended in 5 mM $MgCl_2$ and subsequently diluted 1:1 with 50 mM MES pH 6.0, 400 mM sucrose, 15 mM NaCl and 5 mM $MgCl_2$ and spun down at 3000*g* for 10 min. Resulting pellets were washed in 25 mM MES pH 6.0, 10 mM NaCl and 5 mM $MgCl_2$ and centrifuged at 4500*g* for 10 min. Finally, thylakoids were resuspended in 25 mM MES pH 6.0, 100 mM NaCl, 5 mM $MgCl_2$ and 0.5 M glycine betaine. If not immediately used, thylakoid membranes were flash frozen in liquid nitrogen and stored at −80 °C.

2.5. PSII purification by Ni-NTA affinity chromatography

To isolate His-tag PSII cores, thylakoid membranes of transplastomic plants at a chlorophyll (Chl) concentration of 1 mg mL^{-1} were solubilized with 50 mM n-dodecyl-β-D-maltoside (β-DDM) for 10 min on ice, under gentle stirring. Unsoluble material was removed by two centrifugation steps at 21000*g* for 10 min at 4 °C and the supernatant was loaded on a Ni-NTA column previously pre-equilibrated with a buffer composed of 25 mM MES pH 6.0, 100 mM NaCl, 5 mM $MgCl_2$, 0.5 M glycine betaine, 10 mM imidazole and 0.03% (w/v) β-DDM (equilibration buffer). Binding of the material to the Ni-NTA resin was enhanced through batch loading and incubation for 1 h. After the column had been washed once with the equilibration buffer, further washing continued with a buffer made of 25 mM MES pH 6.0, 100 mM NaCl, 5 mM $MgCl_2$, 0.5 M glycine betaine, 20 mM imidazole and 0.03% (w/v) β-DDM (washing buffer), until the absorbance at 675 nm was below 0.0005. Elution of PSII cores was performed using a buffer with the same composition of the washing buffer, with the exception of an increased imidazole concentration of 250 mM. Eluted PSII particles were washed with a buffer made of 25 mM MES pH 6.0, 100 mM NaCl, 5 mM $MgCl_2$, 1 M glycine betaine, 0.03% (w/v) β-DDM and 10 mM $NaHCO_3$, and finally concentrated by membrane filtration via Amicon Ultra 100 kDa cut-off devices (Millipore) and flash frozen for storage at −80 °C, if not immediately used.

2.6. Spectroscopic analyses

The Chl concentration was measured spectrophotometrically after extraction in 80% (v/v) acetone according to Arnon (1949). Native absorption spectra were recorded using a Lambda25 spectrophotometer (Perkin Elmer) at 12 °C.

2.7. Polyacrylamide gel electrophoresis of proteins and western blotting

Sodiumdodecylsulfate-polyacrylamide gel electrophoresis (SDS-PAGE) was carried out using either the Laemmli's system (Laemmli, 1970) with a 12.5% acrylamide resolving gel containing 5 M urea or the Tris-Tricine system (Schägger, 2006) with a 16% acrylamide resolving gel containing 6 M urea. The separated proteins were either stained by Coomassie brilliant blue R-250 or transferred onto nitro-cellulose membrane and immuno-detected with a specific His-tag antibody (GenScript code A00174), by using the alkaline phosphatase conjugate method, with 5-bromo-4-chloro-3-indolyl phosphate/nitro blue tetrazolium as chromogenic substrates (Sigma-Aldrich). Pre-stained protein size markers (Precision plus, Bio-Rad) were used for the estimation of apparent size of isolated PSII core components. The identity of bands on the SDS-PAGE was assessed by comparing the electrophoretic pattern to that of similar plant PSII preparations obtained in our laboratory and characterized by western blotting or mass spectrometry (Pagliano et al., 2011; Barera et al., 2012).

2.8. Oxygen evolution measurements

The oxygen evolution was measured at 20 °C using a Clark type oxygen electrode (Hansatech) under saturating light intensity (1000 and 5000 μmol m^{-2} s^{-1} photons, respectively for thylakoids and PSII cores). Measurements were performed on three independent replicates in the presence of 0.2 mM 2,6-dichlorobenzoquinone and 2 mM K_3 $[Fe(CN)_6]$ as electron acceptors in 25 mM MES pH 6.5, 5 mM $CaCl_2$, 10 mM NaCl, 10 mM $NaHCO_3$ and 1 M glycine betaine and with Chl concentrations of 10 and 5 μg mL^{-1}, respectively, for isolated thylakoids and PSII cores.

3. Results and discussion

3.1. Development of vectors for the replacement of tobacco native psbB gene with chimeric psbB genes to which a His-tag sequence was added to encode N— or C-terminal His-tagged CP47

Leelavathi and Reddy (2003) successfully used a His-tag based approach for the purification of recombinant proteins accumulated in the chloroplast. In the present study, a similar approach was used to express a chimeric *psbB* gene with a His-tag at N— or C-terminal end of the CP47 protein, a crucial component of the PSII complex. In addition to 8x His-tag, a Gly-linker was introduced to improve the binding of the His-tagged CP47 to Ni-NTA and preserve the PSII complex intactness.

To allow the site-specific recombination required to replace native CP47 with a His-tagged CP47, the genomic region upstream of the *psbB* gene, containing part of the *clpP* coding sequence, was placed flanking the left side of the His-tagged *psbB* and the *psbT*, *psbN*, *psbH* and a partial coding region of *petB* gene flanking the right side of the selection marker *aadA* gene (Fig. 1A). The selectable *aadA* gene was placed downstream to His-tagged *psbB* without disrupting any native gene. The promoter and 5' UTR of native *psbB* were kept intact to allow physiological transcription of the His-tagged *psbB*. A rice derived *psbA* terminator was inserted for efficient termination of transcription, avoiding undesired homologous recombination events. The restriction map of the vectors, possible site-specific recombination sites with the native plastome and the partial chloroplast DNA map of the

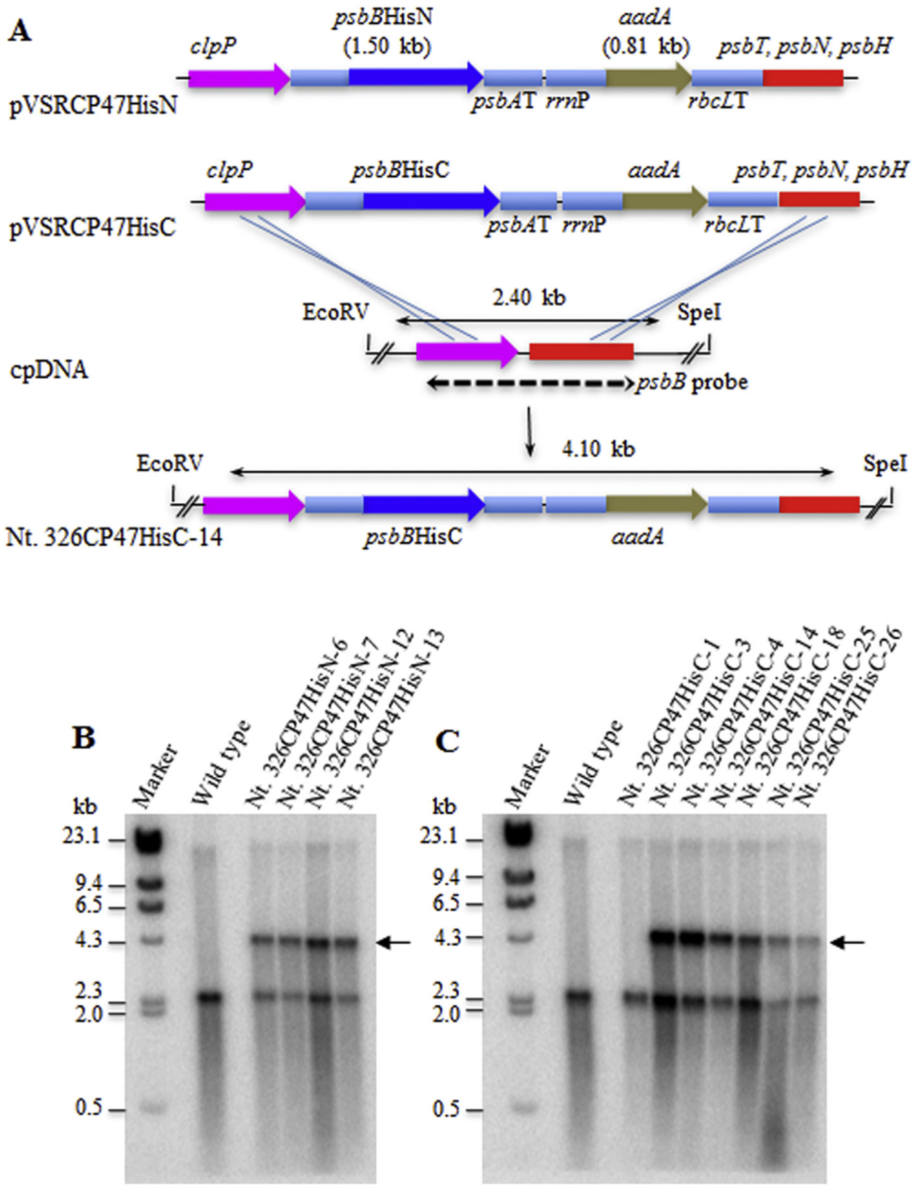

Fig. 1. Introduction of the mutant *psbB* gene into the tobacco plastid genome. (A) Restriction map of vectors pVSRCP47HisN and pVSRCP47HisC, partial chloroplast DNA of tobacco (cpDNA) and the transformed tobacco plant (Nt. 326CP47HisC-14) partial plastid DNA. The *psbB*HisN or *psbB*HisC are under the 5′ expression signals of native *psbB* and 3′ expression signals of rice *psbA*. Lines with double arrow indicate the size of DNA fragments after the restriction digestion with relevant enzymes, EcoRV and SpeI. *psbB* probe (double arrow with dashed line) used in Southern hybridization is also shown. Southern hybridization using *psbB* probe to show site-specific integration of *psbB*HisN (B) and *psbB*HisC (C) into tobacco plastid genome. The arrow indicates the expected size band ~4.0 kb in the transplastomic plants; the ~2.0 kb band corresponds to native tobacco plastome.

transplastomic plant are shown in Fig. 1A.

3.2. Generation of transplastomic tobacco plants containing a modified psbB gene encoding a His-tagged CP47

The particle bombardment of leaf tissue with gold particles coated with pVSRCP47HisN or pVSRCP47HisC plasmid DNA was performed for generating transplastomic plants under spectinomycin selection (Leelavathi et al., 2003). For each construct, about 20–30 green shoots were recovered following spectinomycin selection. In order to achieve homoplasmy of transplastomic plants, three rounds of plant regeneration under spectinomycin selection were carried out.

3.3. Molecular analysis for the stable integration and replacement of native psbB with the modified psbB gene encoding a His-tagged CP47

Southern hybridization was carried out to confirm the stable integration of the chimeric His-tagged *psbB* genes into the plastome of the spectinomycin-resistant lines. Four transplastomic plants obtained from the transformation with pVSRCP47HisN vector were found to contain the transformation cassette when analyzed by Southern blotting. A band of ~4.0 kb in size was observed only in the spectinomycin-resistant lines and was absent in the wild-type plant (Fig. 1B). Similarly, six out of seven plants transformed with pVSRCP47HisC were found to be positive in Southern hybridization. An expected band of ~4.0 kb was present in all the positive plants, while the same sized band was absent in the untransformed wild-type plant (Fig. 1C). These results clearly demonstrate that a sequence encoding a His-tagged CP47 had replaced the sequence encoding the native CP47 in the tobacco plastome. However, a ~2.0 kb band corresponding to native *psbB* was still present in all the transplastomic plants analyzed, suggesting that these plants were still heterotransplastomic despite three cycles of regeneration under spectinomycin selection. Even after a forth cycle of regeneration under same conditions, no homoplasmic line was obtained. A possible explanation is that the native CP47 is able to integrate into the PSII complex more efficiently than the His-tagged CP47, suggesting that PSII complex assembly might be favoring the native gene thus acting as a selective pressure. Nevertheless, more than 50% of the plastome copies in these plants contained the modified *psbB* gene and significant amount of His-tagged CP47 should be expected to be inserted in the PSII complex. This was evident in the pull-down experiments where His-tagged CP47 was able to bind to the Ni-NTA agarose column. Further biochemical and functional analyses showed the presence of an active PSII complex containing His-tagged CP47 protein.

3.4. Characterization of transplastomic plants with a C-term His-tag CP47 subunit

When N-term CP47 His-tag and C-term CP47 His-tag mutants were grown under standard conditions (20 °C, 8 h 150 μmol photons s^{-1} m^{-2} light) on spectinomycin containing medium, a remarkable reduction in the growth rate was observed in the N-term CP47 His-tag mutant (Fig. 2). Since this mutant clearly displayed impaired growth, the C-term tagged mutant, hereafter referred to as CP47 His-tag plant, was chosen for subsequent transfer to the soil. When grown in soil under the same standard conditions, wild-type and CP47 His-tag plants did not show significant differences in the overall morphology, size, and growth rate (data not shown). Oxygen evolution measurements performed on isolated thylakoids to estimate directly the PSII activity, showed similar rates of oxygen evolution both in the His-tagged CP47 mutants and wild-type plants (188 ± 12 *vs.* 183 ± 13 μmol O_2 mg Chl^{-1} h^{-1}), with values comparable to those reported in the literature for higher plants (Pagliano et al., 2011). This demonstrates that the His-tagged complexes are functionally active. The only difference detected between wild-type plants and those expressing His-tagged CP47 was a slightly lower Chl *a*/*b* ratio in the thylakoids of transplastomic plants (3.24 ± 0.18) as compared to that of wild-type tobacco (3.47 ± 0.04), a feature already observed in other His-tagged PSII tobacco plants (Fey et al., 2008).

3.5. Isolation and biochemical characterization of His-tag CP47 PSII cores

Thylakoid membranes from transplastomic tobacco plants were solubilized with β-DDM and loaded on a Ni-NTA column. The His-tag PSII complexes were eluted and checked by western blotting with a specific antibody against the His-tag. This analysis confirmed the recombinant nature of the CP47 His-tag PSII cores of the isolated particles (Fig. 3A). The content of pigment binding protein complexes was evaluated by recording absorption spectra of the isolated particles in the wavelength region from 350 to 750 nm. Fig. 3B shows spectra of CP47 His-tag PSII cores (solid line) and solubilized thylakoids (dashed line), normalized to the maximum in the red region for an easier comparison. Solubilized thylakoids, similarly to flow-through fractions (data not shown), showed the characteristic peaks of Chl *a*, Chl *b* and carotenoids. Structural studies on photosynthetic complexes isolated from higher plants clearly assessed that Chl *b* and high amounts of xanthophylls (lutein, neoxanthin and violaxanthin) are bound to the antenna complexes of both PSI and PSII, but not to their respective cores (Ben-Shem et al., 2003; Liu et al., 2004; Amunts et al., 2007; Umena et al., 2011; Wei et al., 2016). The spectrum of the CP47 His-tag PSII cores showed marked reductions in the absorption of Chl *b* (~647 nm) and xanthophylls (~480 nm) of the antenna complexes, indicative of absence of LHCII polypeptides bound to the cores. These results demonstrate that the protocol developed for the purification allows isolating PSII cores free of outer antenna proteins from thylakoid membranes.

The polypeptide composition of His-tag PSII complexes isolated from mutant plants were investigated by denaturing SDS-PAGE (Fig. 4). This analysis revealed that the isolated PSII particles contained all the main subunits expected in a plant PSII core: the intrinsic subunits D1 and D2 of the reaction centre, the inner antenna proteins CP47 and CP43, and the extrinsic polypeptides PsbO, PsbP and PsbQ. In addition, some small subunits were visible in the low molecular mass region of the Tris-Tricine SDS-PAGE (Fig. 4), suggesting the presence of a full complement of low molecular mass PSII subunits in this preparation. However, a

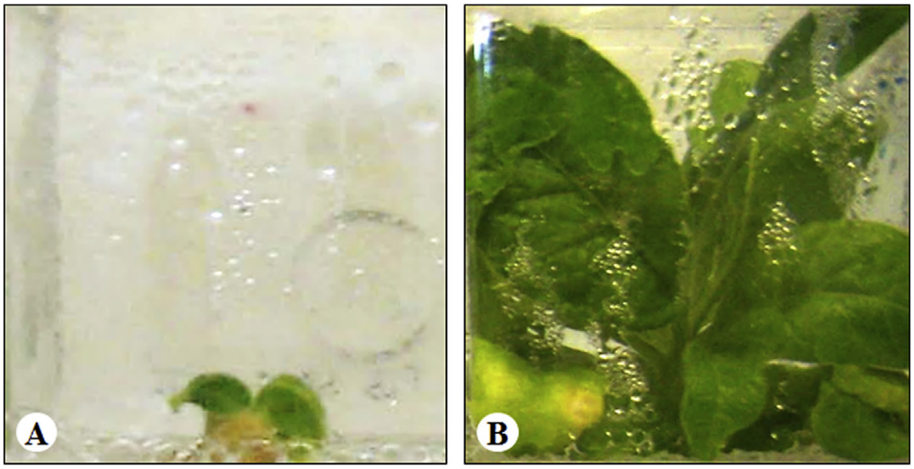

Fig. 2. Visual phenotype of CP47 His-tag tobacco mutants. N-term CP47 His-tag (A) and C-term CP47 His-tag (B) tobacco mutants inside culture boxes at the end of the third regeneration cycle on spectinomycin (500 mg L^{-1}) containing medium.

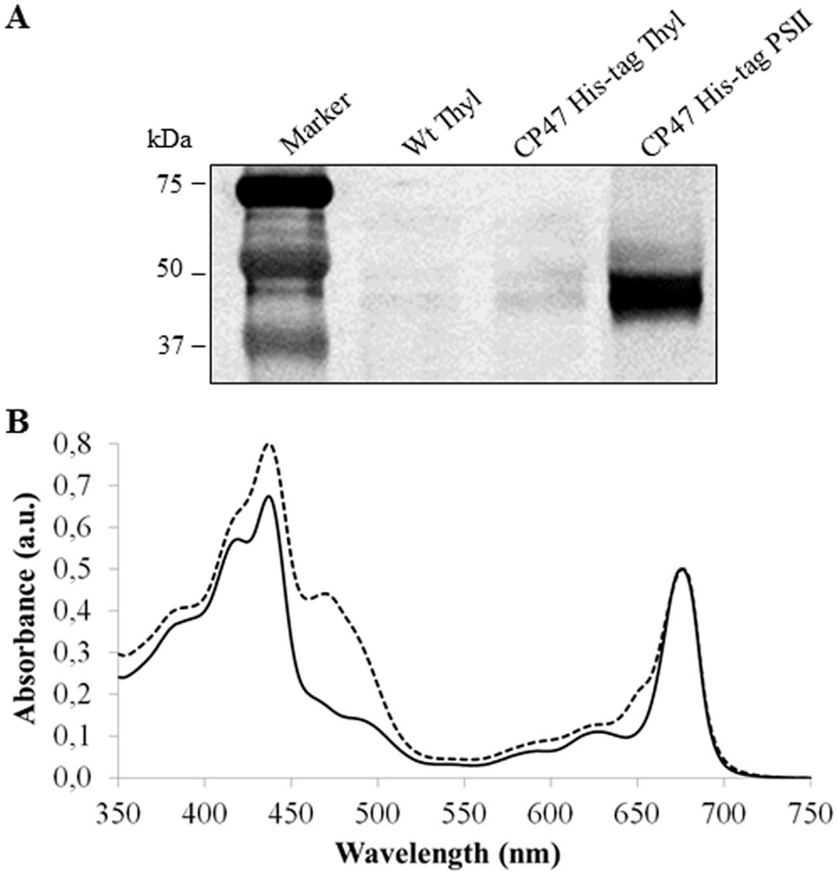

Fig. 3. Western blot analysis and absorption spectrum of the PSII cores isolated from CP47 His-tag tobacco mutants. (A) Western blot analysis using the His-tag antibody of wild-type thylakoids (Wt Thyl), CP47 mutant thylakoids (CP47 His-tag Thyl) and PSII cores isolated by Ni-NTA affinity chromatography from CP47 mutant thylakoids solubilized with β-DDM (CP47 His-tag PSII). 5 μg Chl for thylakoids and 1 μg Chl for PSII were loaded on a SDS-PAGE performed according to Laemmli's system (Laemmli, 1970). *Marker*, pre-stained protein markers (Precision plus, Bio-Rad) with their apparent molecular weight (kDa) indicated. (B) Absorption spectrum of CP47 His-tag PSII cores (solid line) isolated by Ni-NTA affinity chromatography and, for comparison, a spectrum of solubilized thylakoids (dashed line) loaded onto the chromatographic column. Spectra are normalized to the maximum in the red region.

certain amount of some polypeptides not belonging to PSII was found in the sample. Based on their positioning on the gel, and on earlier reports about impurities using the Ni-NTA technique with thylakoid membranes (Fey et al., 2008), they likely correspond to PSI and ATP-synthase subunits that have a natural affinity for the matrix. Despite such impurities, the purification protocol adopted in this work succeeded in the isolation of His-tag PSII core complexes functionally active, as demonstrated by the rate of oxygen evolution measured around 516 ± 28 μmol O_2 mg Chl^{-1} h^{-1}. This value is comparable with activities displayed by some PSII cores preparations obtained from other His-tagged PSII tobacco plants (Fey et al., 2008). Considering the direct involvement of the inner antenna protein CP47 in the energy transfer pathway within PSII (Wei et al., 2016), such high rate of oxygen evolution indicates that the insertion of the His-tag operated at the C-term of CP47 does not interfere with its native folding and binding to the reaction centre subunits and ultimately does not compromise the photocatalytic activity of the PSII core in the transplastomic plants. These results demonstrate that the isolated His-tag PSII core complexes are suitable for further functional and structural analyses requiring fully active preparations, such as spectroscopic measurements and single-particle cryo-electron microscopy, which are still needed to thoroughly elucidate the structure-function relationships of PSII in higher plants. For instance, CP47 His-tag PSII particles retaining the full complement of OEC subunits isolated from dark-adapted and illuminated plants could be used for cross-linking experiments of the extrinsic subunits in combination with single-particle cryo-electron microscopy for high-resolution probing of local conformational changes expected to occur in the flexible regions of PsbP and PsbQ when they bind to the PSII core in an active catalytic state, ultimately contributing to the understanding of the water-splitting reaction and its environment in higher plants.

3.6. *Yield of extraction*

In higher plant thylakoids, the PSII/PSI stoichiometry varies roughly between 1 and 2.5, depending on light quality differences during plant growth (Fan et al., 2007). Within PSII, the majority of the Chl molecules are not bound to the PSII core in vivo, but to LHCII peripheral antenna complexes. The plant PSII core contains 35 Chl per reaction centre (Wei et al., 2016), and the total Chl per PSII reaction centre is considered to be around 600, depending on plant growth light conditions (Wild et al., 1986). Thus, the maximal yield of PSII cores, which can be expected in terms of chlorophyll, is only around 6%. In our preparations, approximately 0.25% of chlorophyll of the starting thylakoids was retrieved in the purified His-tag PSII cores, thus we can estimate a yield of about 4% of pure PSII cores. The molecular tool developed for isolating PSII from *N. tabacum* described in this work could provide a one-step method of purification of functional PSII cores directly from thylakoid membranes, alternative to longer and less efficient procedures (i.e., sucrose

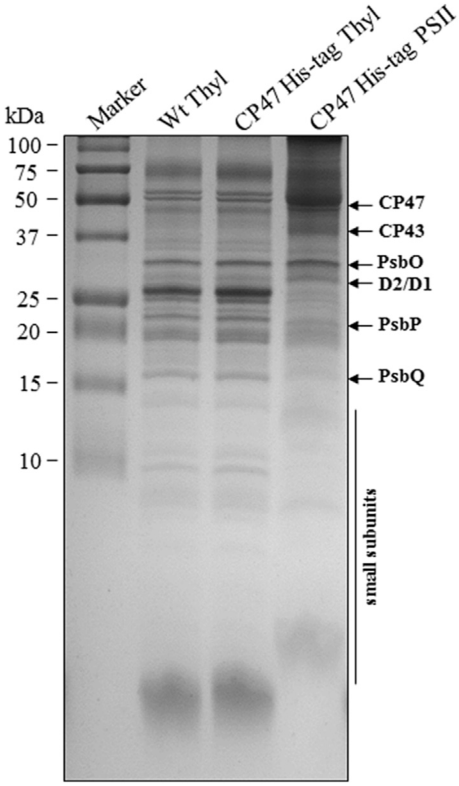

Fig. 4. SDS-PAGE of the PSII cores isolated from CP47 His-tag tobacco mutants. Coomassie stained Tris-Tricine SDS-PAGE performed according to Schägger (2006) of wild-type thylakoids (Wt Thyl), CP47 mutant thylakoids (CP47 His-tag Thyl) and PSII cores isolated by Ni-NTA affinity chromatography from CP47 mutant thylakoids solubilized with β-DDM (CP47 His-tag PSII). 10 μg Chl were loaded for thylakoids and 5 μg Chl were loaded for PSII. *Marker*, pre-stained protein markers (Precision plus, Bio-Rad) with their apparent molecular weight (kDa) indicated.

density gradient ultracentrifugation), that can be applied on a routine basis for studying structural and functional aspects of PSII in higher plants.

4. Conclusions

A successful attempt has been made to express a His-tagged CP47 protein in tobacco chloroplasts through genetic transformation approach. C-term His-tag CP47 plants did not show significant differences in growth parameters and overall morphology with respect to wild-type plants. The C-term His-tagged CP47 subunit has been found to integrate itself into the PSII core complex. Pull-down experiments using Ni-NTA affinity chromatography, protein profile analysis and steady state oxygen evolution measurements showed the feasibility of isolating an intact and functional PSII core complex with a His-tag CP47 subunit from transplastomic tobacco plants. These findings may open up new opportunities to elucidate further structural and functional aspects of the PSII complex from higher plants.

Contributions

LB, PL, and LP designed and prepared vectors for the transformation. LB, AD and SL generated the transplastomic plants and carried out Southern blot analysis. CP performed the isolation and biochemical characterization of PSII core complexes. RC and VSR conceived and supervised the study. CP, VSR and RC wrote the article. All authors reviewed the results and approved the final version of the manuscript.

Acknowledgements

Part of this work was made possible via a ICGEB Fellowship to LB. This work received internal financial support by DBT and ICGEB. The authors kindly thank Dr Fabiana Chimirri (Politecnico di Torino, Italy) for the considerable efforts in the initial experiments and technical support to CP with PSII cores purification.

Appendix A. Supplementary data

Supplementary data related to this article can be found at http://dx.doi.org/10.1016/j.plaphy.2016.12.009.

References

Amunts, A., Drory, O., Nelson, N., 2007. The structure of a plant photosystem I supercomplex at 3.4 Å resolution. Nature 447, 58–63. http://dx.doi.org/10.1038/nature05687.

Arnon, D.I., 1949. Copper enzymes in isolated chloroplasts. Polyphenoloxidase in *Beta vulgaris*. Plant Physiol. 24, 1–15.

Balsera, M., Arellano, J.B., Revuelta, J.L., de las Rivas, J., Hermoso, J.A., 2005. The 1.49 Å resolution crystal structure of PsbQ from photosystem II of *Spinacia oleracea* reveals a PPII structure in the N-terminal region. J. Mol. Biol. 350, 1051–1060. http://dx.doi.org/10.1016/j.jmb.2005.05.044.

Barbato, R., Friso, G., Rigoni, F., Dalla Vecchia, F., Giacometti, G.M., 1992. Structural changes and lateral redistribution of photosystem II during donor side photoinhibition of thylakoids. J. Cell Biol. 119, 325–335.

Barera, S., Pagliano, C., Pape, T., Saracco, G., Barber, J., 2012. Characterization of PSII-LHCII supercomplexes isolated from pea thylakoid membrane by one-step treatment with α- and β-dodecyl-D-maltoside. Philos. Trans. R. Soc. Lond. B. Biol. Sci. 367, 3389–3399. http://dx.doi.org/10.1098/rstb.2012.0056.

Ben-Shem, A., Frolow, F., Nelson, N., 2003. Crystal structure of plant photosystem I. Nature 426, 630–635. http://dx.doi.org/10.1038/nature02200.

Bricker, T.M., Morvant, J., Masri, N., Sutton, H.M., Frankel, L.K., 1998. Isolation of a highly active photosystem II preparation from *Synechocystis* 6803 using a histidine-tagged mutant of CP 47. Biochim. Biophys. Acta 1409, 50–57.

Calderone, V., Trabucco, M., Vujičić, A., Battistutta, R., Giacometti, G.M., Andreucci, F., Barbato, R., Zanotti, G., 2003. Crystal structure of the PsbQ protein of photosystem II from higher plants. EMBO Rep. 4, 900–905. http://dx.doi.org/10.1038/sj.embor.embor923.

Danielsson, R., Suorsa, M., Paakkarinen, V., Albertsson, P.-A., Styring, S., Aro, E.-M., Mamedov, F., 2006. Dimeric and monomeric organization of photosystem II. Distribution of five distinct complexes in the different domains of the thylakoid membrane. J. Biol. Chem. 281, 14241–14249. http://dx.doi.org/10.1074/jbc.M600634200.

Fan, D.-Y., Hope, A.B., Smith, P.J., Jia, H., Pace, R.J., Anderson, J.M., Chow, W.S., 2007. The stoichiometry of the two photosystems in higher plants revisited. Biochim. Biophys. Acta 1767, 1064–1072. http://dx.doi.org/10.1016/j.bbabio.2007.06.001.

Fey, H., Piano, D., Horn, R., Fischer, D., Schmidt, M., Ruf, S., Schröder, W.P., Bock, R., Büchel, C., 2008. Isolation of highly active photosystem II core complexes with a His-tagged Cyt b559 subunit from transplastomic tobacco plants. Biochim. Biophys. Acta 1777, 1501–1509. http://dx.doi.org/10.1016/j.bbabio.2008.09.012.

Hankamer, B., Nield, J., Zheleva, D., Boekema, E., Jansson, S., Barber, J., 1997. Isolation and biochemical characterization of monomeric and dimeric photosystem II complexes from spinach and their relevance to the organization of photosystem II in vivo. Eur. J. Biochem. FEBS 243, 422–429.

Hankamer, B., Morris, E.P., Barber, J., 1999. Revealing the structure of the oxygen-evolving core dimer of photosystem II by cryoelectron crystallography. Nat. Struct. Biol. 6, 560–564. http://dx.doi.org/10.1038/9341.

Hankamer, B., Morris, E., Nield, J., Gerle, C., Barber, J., 2001. Three-dimensional structure of the photosystem II core dimer of higher plants determined by electron microscopy. J. Struct. Biol. 135, 262–269. http://dx.doi.org/10.1006/jsbi.2001.4405.

Ifuku, K., Nakatsu, T., Kato, H., Sato, F., 2004. Crystal structure of the PsbP protein of photosystem II from *Nicotiana tabacum*. EMBO Rep. 5, 362–367. http://dx.doi.org/10.1038/sj.embor.7400113.

Johnson, E.A., Rosenberg, J., McCarty, R.E., 2007. Expression by *Chlamydomonas reinhardtii* of a chloroplast ATP synthase with polyhistidine-tagged beta subunits. Biochim. Biophys. Acta 1767, 374–380. http://dx.doi.org/10.1016/j.bbabio.2007.03.003.

Kashino, Y., Lauber, W.M., Carroll, J.A., Wang, Q., Whitmarsh, J., Satoh, K., Pakrasi, H.B., 2002. Proteomic analysis of a highly active photosystem II preparation from the cyanobacterium *Synechocystis* sp. PCC 6803 reveals the presence of novel polypeptides. Biochem. (Mosc.) 41, 8004–8012.

Laemmli, U.K., 1970. Cleavage of structural proteins during the assembly of the head of bacteriophage T4. Nature 227, 680–685.

Leelavathi, S., Reddy, V.S., 2003. Chloroplast expression of His-tagged GUS-fusions: a general strategy to overproduce and purify foreign proteins using transplastomic plants as bioreactors. Mol. Breed. 11, 49–58. http://dx.doi.org/10.1023/A:1022114427971.

Leelavathi, S., Gupta, N., Maiti, S., Ghosh, A., Reddy, V.S., 2003. Overproduction of an alkali- and thermo-stable xylanase in tobacco chloroplasts and efficient recovery of the enzyme. Mol. Breed. 11, 59–67. http://dx.doi.org/10.1023/A:1022168321380.

Liu, Z., Yan, H., Wang, K., Kuang, T., Zhang, J., Gui, L., An, X., Chang, W., 2004. Crystal structure of spinach major light-harvesting complex at 2.72 Å resolution. Nature 428, 287–292. http://dx.doi.org/10.1038/nature02373.

Pagliano, C., Chimirri, F., Saracco, G., Marsano, F., Barber, J., 2011. One-step isolation and biochemical characterization of a highly active plant PSII monomeric core. Photosynth. Res. 108, 33–46. http://dx.doi.org/10.1007/s11120-011-9650-4.

Pagliano, C., Saracco, G., Barber, J., 2013. Structural, functional and auxiliary proteins of photosystem II. Photosynth. Res. 116, 167–188. http://dx.doi.org/10.1007/s11120-013-9803-8.

Pan, X., Li, M., Wan, T., Wang, L., Jia, C., Hou, Z., Zhao, X., Zhang, J., Chang, W., 2011. Structural insights into energy regulation of light-harvesting complex CP29 from spinach. Nat. Struct. Mol. Biol. 18, 309–315. http://dx.doi.org/10.1038/nsmb.2008.

Rhee, K.H., Morris, E.P., Barber, J., Kühlbrandt, W., 1998. Three-dimensional structure of the plant photosystem II reaction centre at 8 Å resolution. Nature 396, 283–286. http://dx.doi.org/10.1038/24421.

Sambrook, J., Maniatis, T., Fritsch, E.F., 1989. Molecular Cloning: a Laboratory Manual. Volumes 1 and 2. Cell 61, 17–18 In: Current Protocols in Molecular Biology, second ed., vol. 1–3. http://dx.doi.org/10.1016/0092-8674(90)90210-6

Schägger, H., 2006. Tricine-SDS-PAGE. Nat. Protoc. 1, 16–22. http://dx.doi.org/10.1038/nprot.2006.4.

Shen, J.-R., 2015. The structure of Photosystem II and the mechanism of water oxidation in photosynthesis. Annu. Rev. Plant Biol. 66, 23–48. http://dx.doi.org/10.1146/annurev-arplant-050312-120129.

Shi, L.-X., Schröder, W.P., 2004. The low molecular mass subunits of the photosynthetic supracomplex, photosystem II. Biochim. Biophys. Acta 1608, 75–96. http://dx.doi.org/10.1016/j.bbabio.2003.12.004.

Shi, L.-X., Hall, M., Funk, C., Schröder, W.P., 2012. Photosystem II, a growing complex: updates on newly discovered components and low molecular mass proteins. Biochim. Biophys. Acta 1817, 13–25. http://dx.doi.org/10.1016/j.bbabio.2011.08.008.

Standfuss, J., Terwisscha van Scheltinga, A.C., Lamborghini, M., Kühlbrandt, W., 2005. Mechanisms of photoprotection and nonphotochemical quenching in pea light-harvesting complex at 2.5 Å resolution. EMBO J. 24, 919–928. http://dx.doi.org/10.1038/sj.emboj.7600585.

Suzuki, T., Minagawa, J., Tomo, T., Sonoike, K., Ohta, H., Enami, I., 2003. Binding and functional properties of the extrinsic proteins in oxygen-evolving photosystem II particle from a green alga, *Chlamydomonas reinhardtii* having his-tagged CP47. Plant Cell Physiol. 44, 76–84.

Umena, Y., Kawakami, K., Shen, J.-R., Kamiya, N., 2011. Crystal structure of oxygen-evolving photosystem II at a resolution of 1.9 Å. Nature 473, 55–60. http://dx.doi.org/10.1038/nature09913.

Wei, X., Su, X., Cao, P., Liu, X., Chang, W., Li, M., Zhang, X., Liu, Z., 2016. Structure of spinach photosystem II-LHCII supercomplex at 3.2 Å resolution. Nature 534, 69–74. http://dx.doi.org/10.1038/nature18020.

Wild, A., Höpfner, M., Rühle, W., Richter, M., 1986. Changes in the stoichiometry of photosystem II components as an adaptive response to high-light and low-light conditions during growth. Z. Naturforsch 41c, 597–603.